Theoretical Study of Cisplatin Binding to DNA: The Importance of Initial Complex Stabilization

Johan Raber,[†] Chuanbao Zhu,[‡,§] and Leif A. Eriksson*[,‡]

Department of Cell and Molecular Biology, Uppsala University, Box 596, 751 24 Uppsala, Sweden, and Department of Natural Sciences, Örebro University, 701 82 Örebro, Sweden

Received: January 5, 2005; In Final Form: April 1, 2005

The first and second substitution reactions between activated (hydrolyzed) cisplatin, $Pt(NH_3)_2(H_2O)_2^{2+}$, and purine bases guanine and adenine are explored using the B3LYP hybrid functional, IEF−PCM solvation models, and large basis sets. The computed free energy barrier for the first substitution is 19.5 kcal/mol for guanine (exptl value = 18.3 kcal/mol) and 24.0 kcal/mol for adenine. The observed predominance toward guanine in the first substitution is explained in terms of significantly larger stabilization energy for the initially formed complex, compared with adenine, in combination with favored kinetics, and represents a revised view of the proposed mechanism for cisplatin binding to DNA. For the second substitution, the computed barrier for $Pt(NH_3)_2G_2^{2+}$ head-to-head formation is 22.5 kcal/mol, in very good agreement with experimental data for adduct closure (23.4 kcal/mol). Again, a higher stability in complexation with G over A is ascribed as the main contributing factor favoring G over A substitution. The calculations provide a first explanation for the predominance of 1,2-d(GpG) over 1,2-d(ApG) intrastrand didentate adducts, and the origin of the 5′−3′ direction specificity of the 1,2-d(ApG) adducts.

Introduction

One of the biggest success stories in cancer treatment is the discovery by Rosenberg et al.[1] of the antitumor properties of the square planar compound cisplatin, or *cis*-diamminedichloroplatinum(II) (cis-DDP). In the four decades passed since, relatively few cisplatin derivatives have been released on the market and they are generally active against the same spectrum of tumors as the parent compound, mainly ovarian, testicular, head, and neck cancers.[2,3] Improvements to the drug have so far been limited to enabling oral administration and reducing toxicity (that is, carboplatin), thereby permitting outpatient treatment.[4] Derivative drugs oxaliplatin and nedaplatin have received approval in France and Japan, respectively.[5] The second-generation compound carboplatin, although significantly less toxic than cisplatin, unfortunately displays cross-resistance toward the same range of tumors as cisplatin. All of the above compounds abide to the original set of structure−activity relationship (SAR) rules determined by Cleare and Hoeschele[6,7] and Reedijk,[8] stating that the platinum compound has to be neutral with the N-donor ligands in the cis conformation and to have at least one N−H moiety in them. They should furthermore have leaving groups with lability in a "window of reactivity" approximately centered on chloride. Recent research however, focuses on radically different platinum compound topologies including polynuclear species and hexacoordinated Pt(IV) complexes, as these seem to avoid resistance mechanisms of the cell induced by cisplatin treatment.[9]

The cisplatins clinical target has, in a number of studies, been shown to be cellular DNA,[10−12] to which it forms several different didentate adducts. The most notable ones are the intrastrand didentate adducts 1,2-d(GpG) at ∼65% of the total amount of adducts, and 1,2-d(ApG) at ∼25%.[13,14] These adducts have also been pointed out as the ones correlating to the antitumor properties of cisplatin since they are not formed by the clinically inactive geometric isomer transplatin,[15] although this view is not unchallenged. Other adducts formed are the intrastrand 1,3-d(GpNpG) (N being any base), the interstrand GG adduct, monofunctional adducts to guanine, and various DNA protein adducts. It is worth noting that neither monofunctional adducts to adenine nor interstrand AG adducts have been detected, the reason for which is unknown.

All didentate adducts to DNA cause a localized unwinding of the duplex and a widening of the minor groove, but with major differences between the intra- and interstrand adducts.[16,17] Apart from the duplex unwinding, the major platination product, 1,2-d(GpG), introduces a kink to the DNA molecule toward the major groove and opens a hydrophobic pocket in the minor groove between the two guanine bases. This kink, and the widened minor groove with the hydrophobic pocket, provides a motif of recognition for a class of proteins called "HMG-domain proteins".[18,19]

Although no structural data are available for 1,2-d(ApG), there is strong reason to believe that this didentate adduct should closely resemble that of 1,2-d(GpG). This is further supported by findings that HMG-domain proteins also recognize and form a complex with this adduct.[20] The 1,2-d(ApG) adduct is direction-specific, 5′−3′, and no explanation for this directionality has to our knowledge been given.

There are two types of conformations of bifunctional adducts: the head-to-head (HH) in which both O_6/N_6 of the nucleotides are located on the same side of the platinum coordination plane, and the head-to-tail (HT) arrangement where they reside on opposite sides of the plane. The head-to-head

* Corresponding author. Fax: 46 19 303 566. E-mail: leif.eriksson@nat.oru.se.
[†] Uppsala University.
[‡] Örebro University.
[§] Current address: Department of Chemistry and Biochemistry, University of Windsor, Windsor, Ontario, N9B 3P4 Canada.

10.1021/jp050057d CCC: $30.25 © 2005 American Chemical Society
Published on Web 05/04/2005

arrangement is observed for the intrastrand bifunctional adducts, while the head-to-tail arrangement corresponds to the interstrand adducts.

Prior to cisplatin attack on DNA, one or two hydrolyzations take place substituting the chloride ligands by water. This occurs when cisplatin passes from the relatively high chloride concentration of the blood plasma to the lower concentration of the cell cytoplasm. The most common view is that only one chloride is hydrolyzed before the attack on DNA,[21,22] based on kinetic data for the hydrolyzation process in solutions with low chloride concentration. A conflicting view has been put forward, however,[23] pointing out the ratio of 1,2-d(ApG) to 1,2-d(GpG) adducts found in in-vitro studies (ratio 1:3) of cisplatin−DNA bond formation as being better reproduced by exposure to diaquated than monoaquated cisplatin.

One may ask whether the preference of platination toward guanine over adenine is manifested in the chemical differences of the purines, or if this bias is due to steric and other electronic effects imposed by the adjoining parts of DNA. Furthermore, the role played by the carrier ligands of cisplatin (NH_3) is largely unresolved; the SAR-implied importance of at least one −NH moiety in the ammine suggests crucial hydrogen bonding.

Substitution reactions in square planar compounds have been investigated intensively on a number of different complexes including several different metal ions and ligands.[24] Ligand substitutions in square planar complexes proceed via trigonal bipyramidal transition states from reactant to product.[25]

Many different aspects of cisplatin−DNA interactions have been investigated at a theoretical level, including effects on base-pairing due to platination[26] and the influence of the DNA backbone on the cisplatin−DNA adduct.[27,28] The hydrogen-bonding influence on the stability of mono- and bifunctional adducts has been studied[29] as well as kinetic factors governing the competition between nitrogen and sulfur ligands in cisplatin binding.[30] Further aspects of cisplatin binding to DNA have been examined in Car-Parinello MD calculations[31] investigating the structure of a GpG−cisplatin didentate adduct in water.

Structures obtained through DFT calculations have been reported showing the geometry of cisplatin substituted by one or two purines[32] along with estimates of bond dissociation energies. Of more immediate interest to this study is the work of Baik et al.[33] in which the first substitution of activated cisplatin with isolated purine bases was examined using density functional theory. In that study, the substitution energy profiles were reported for both monoaquated and diaquated cisplatin with both adenine and guanine as the substituting agent, wherein good agreement with available experimental data was found. However, the study reported only transition state and product complex geometries but no optimized reactant complex geometries for the substitutions in question. This leaves room for some doubt regarding the accuracy of the activation energy barriers reported.

Several theoretical studies have also been published on the related topic of cisplatin activation reactions, detailing the substitution reactions wherein the chloride ligands are sequentially substituted by water molecules, studies which suggest trigonal bipyramidal transition states for these substitution reactions.[34−38]

In this work, the reaction energy profiles for the first and second substitution reactions of diaquated cisplatin with adenine and guanine nucleotides are presented. The choice of diaquated cisplatin, rather than monoaquated, as the activated state of cisplatin is motivated by the experimental evidence that the ratio of adducts to DNA formed by diaquated cisplatin closely follow the ratio observed. The role of initial complex stabilization in governing the system toward observed products is discussed on the basis of the results of the calculations, and a suggestion for the origin of the direction specificity of the 1,2-d(ApG) products is presented.

Methods

All geometry optimizations were done in the gas phase using the Becke three-parameter hybrid exchange functional[39] (B3) and the Lee, Yang, and Parr correlation functional[40] (LYP) in combination with the LanL2DZ[41−43] effective core potential basis set for the platinum atom, whereas all other atoms were described using the 6-31G(d,p) Pople basis set. This level of theory was also used for the vibrational frequency calculations. Single-point calculations were performed at the B3LYP/(LanL2DZ + 6-311+G(2d,2p)) level of theory. The reactant and product complexes were obtained by following the intrinsic reaction coordinate[44,45] of the corresponding transition state in both directions of the reaction path, followed by standard geometry optimizations. Minima and saddle points along the reaction coordinate were verified by frequency calculations. Thermal energy contributions were extracted from the frequency calculations to obtain the respective Gibbs free energies at 298 K. Solvent effects were accounted for by means of single-point calculations on all stationary structures with a polarizable continuum model, IEF−PCM.[46,47,48] The dielectric constant of water ($\epsilon_{wat} = 78.39$) was used to approximate the bulk effects of solvation.

In the first and second substitution reactions, counterpoise (CP) calculations[49,50] were conducted on the reactant complex with lowest energy to find an estimate of the basis set superposition error (BSSE), ΔE_{CP}. The obtained BSSE estimates were subsequently used to calculate complexation energies according to the formula:

$$\Delta E_{\text{complexation}} = E_{\text{RC}}(\text{cPt-purine})^{*} - E(\text{cPt}) - E(\text{purine}) + \Delta E_{\text{CP}}$$

The asterisk denotes the optimized RC geometry, and the lack thereof denotes the optimized geometry of the isolated reactant. ΔE_{CP} is calculated for the RC geometry. The energies used in this calculation are Gibbs free energies including solvation corrections.

The second substitution was followed in the order it would occur in-vitro/vivo, that is, with the second reactant being either adenine or guanine, adding to either of the two cisplatin−guanine product complexes. The current work is a continuation of our ongoing studies of the chemistry cisplatin and its derivatives.[38,51] All calculations were performed using the Gaussian 03 program package.[52]

Results and Discussion

The reactions leading to the didentate adduct have in the current calculations been considered separately, that is, only the moieties directly involved in the substitution are included in each reaction step. The convention used for naming the ligands of platinum and other atoms of interest is as follows: N7 for the binding nitrogen of the attacking purine ligand, H_2O for the leaving ligand, and L_{ax1} for the ligand hydrogen-bonded to O_6/N_6 of the attacking purine at the corresponding transition state. The labeling of atoms in the purines follows the established convention.

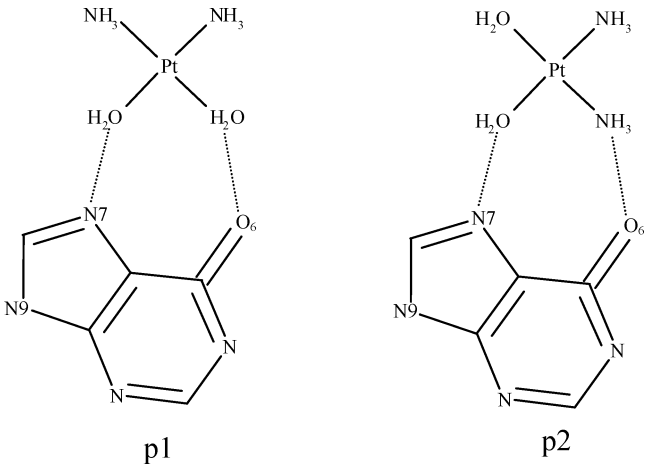

Figure 1. Schematic drawing of the two hydrogen-bond patterns between the reactants (shown here: guanine) of the first substitutions found to have associated transition states and product complexes.

The stationary points obtained are in the absence of the surrounding DNA bases and backbone, and it is therefore likely that the absolute energies obtained may deviate slightly from the actual case, that is, steric effects and the effects of the phosphoribose bridges are not included. It is reasonable to assume, however, considering the large similarities of the stationary point geometries, that these effects are similar in magnitude for the reaction paths studied here.

The First Substitution. The hydrogen-bond donors of activated cisplatin enable the drug to form stable complexes through interactions with the hydrogen-bond acceptors of the purine bases exposed in the major groove of DNA, that is, the purine N7 and the O_6 oxo or N_6 amine groups, respectively. In this study, two cisplatin−purine hydrogen-bond patterns were found, leading to distinct transition states. These are labeled p1 and p2, to distinguish between the two paths of the reactions. In p1, hydrogen bonds are formed from N7 and O_6/N_6 to the cisplatin water ligands. In p2, there is a cisplatin ammine−O_6/N_6 hydrogen bond and a water−N7 hydrogen bond, schematically illustrated in Figure 1. The cisplatin moiety is in all the reactant and product complexes square planar with respect to its primary ligand atoms, and the transition states trigonal bipyramids.

The +2 charge of diaquated cisplatin indirectly gives rise to proton transfer from the cisplatin moiety to the substituting purine base in some of the calculated stationary states of the first substitution (see Figures 2 and 3). For all reactant complexes (RC), proton transfer between a water ligand and N7 of the purine was observed, whereas for the substitution of adenine in path 1 (A•p1) also the remaining stationary points displayed full proton transfers from cisplatin to the adenine, as evident in Figure 2. A likely cause of this effect is that the geometry optimizations are performed in the gas phase on the +2 cationic metal−ligand complexes. Thereby the protons of the water ligands become more acidic than would be the case in an aqueous environment. There are, to our knowledge, no experimental indications that proton transfer to N7 prior to cisplatin bonding to DNA is present. Instead, protonation of N7 (if a separate reaction step) is a step in acid-catalyzed depurination of DNA and would in vivo likely break the purine *N*-glycosyl bond.[53−56] In the current reactions, however, protonation occurs during the initiation of the reaction between the purine and cisplatin and cannot be considered an isolated reaction step.

The proton transfers give rise to minor modifications in the geometric structures of the partaking components. The largest changes are seen for the cisplatin moiety, where the bond distance between the deprotonated water and platinum is reduced by ∼0.1 Å (from 2.13 to 2.03 Å) compared to the separately optimized structure of diaquated cisplatin. Consequently the bond length of the ammine ligand in trans position increases by ∼0.06 Å (from 2.05 to 2.11 Å) with respect to the separately optimized structure. The effect of the protonation on the attacking purine is minor (in general, ca. 0.01 Å).

The energies of the reactant complexes for the two types of conformers found (see Figure 1) reveal that these are not equally stable. This is to be expected given that the hydrogen bonds formed between the different groups are not of equal strength. The magnitude of this energy difference in the gas phase is −3.4 kcal/mol for adenine (ΔG = A•p1 − A•p2) and −4.4 kcal/mol for guanine (ΔG = G•p1 − G•p2). With solvation model included, the corresponding ΔG values are −1.3 and −2.6 kcal/mol.

To compare the complexation energies for the different substituents, counterpoise calculations were performed on G•p1 and A•p1. These calculations showed the G•p1 to be more stable than A•p1 by 7.8 kcal/mol. Analysis of the constituent energy contributions to this energy difference revealed two main contributions: solvation and electronic energy. The BSSE energy correction and the vibrational energy contributions are of similar magnitude for the complexes and their isolated constituents. The solvation energy contribution favors the A•p1 RC by 7.3 kcal/mol, while the electronic contribution to the complexation energy is 14.2 kcal/mol lower for G•p1. The relative energies of the different reaction paths are shown in Figure 4, and the absolute energies are given in Table 1.

The different transition states (TS) display large geometrical similarities. This is expected since the ligands involved are much alike, that is, the leaving ligand is in all cases water, the entering ligand is a purine and the ligand positioned trans to the leaving water ligand is an ammine group. However, in the transition states of path 1 for both adenine and guanine, proton transfer is observed between the axial water ligand (L_{ax1}) and N_6/O_6. In the adenine case we observe a complete proton transfer to the N_6 moiety of the purine, whereas in the guanine case it is best described as a partial transfer to O_6 (see Figure 2). Similar partial proton transfer in the G•p1 TS has been reported as supplementary information in a previous theoretical study by Baik et al.,[33] whereas the proton transfer in the A•p1 TS was not reported even though the same exchange-correlation functional and basis set were used as in the current work. Attempts were made to manually move the proton back to the cisplatin moiety to rule out the possibility that the proton transfers were a computational artifact. However, the subsequent geometry reoptimizations reproduced our initial result with full or partial proton transfers.

Without exception, the imaginary frequencies of these TSs are of low magnitude, 147i−151i cm^{-1}, indicating a flat PES along the reaction coordinate at the geometry of the TS. The leaving ligand is in all cases the water molecule hydrogen-bonded to the purine N7 in its associated RC.

The most notable geometrical differences between the TSs of the two paths is caused by the proton transfer observed in path 1 but not in path 2. This is reflected in that the distance between the L_{ax1} ligand and O_6/N_6 is significantly shorter in path 1 TSs than in path 2 TSs (2.40, 2.54, 2.65 and 2.85 Å for the G•p1, A•p1, G•p2, and A•p2 TSs, respectively). Another distinguishing geometrical feature between the paths is the

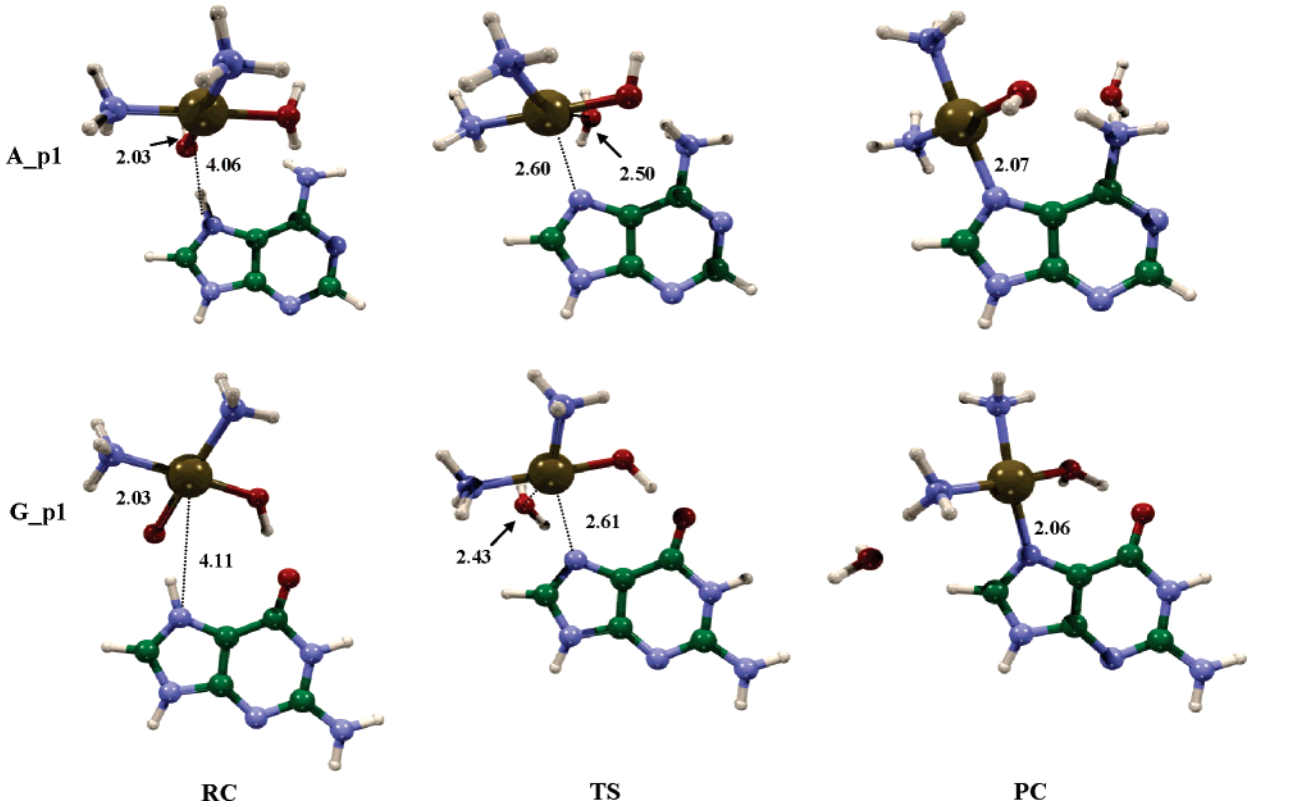

Figure 2. Stationary points (RC, TS, and PC) along the reaction coordinate of the first substitution path 1. Top row shows the substitution of a cisplatin water ligand by adenine, and bottom row shows the substitution with guanine as the attacking ligand.

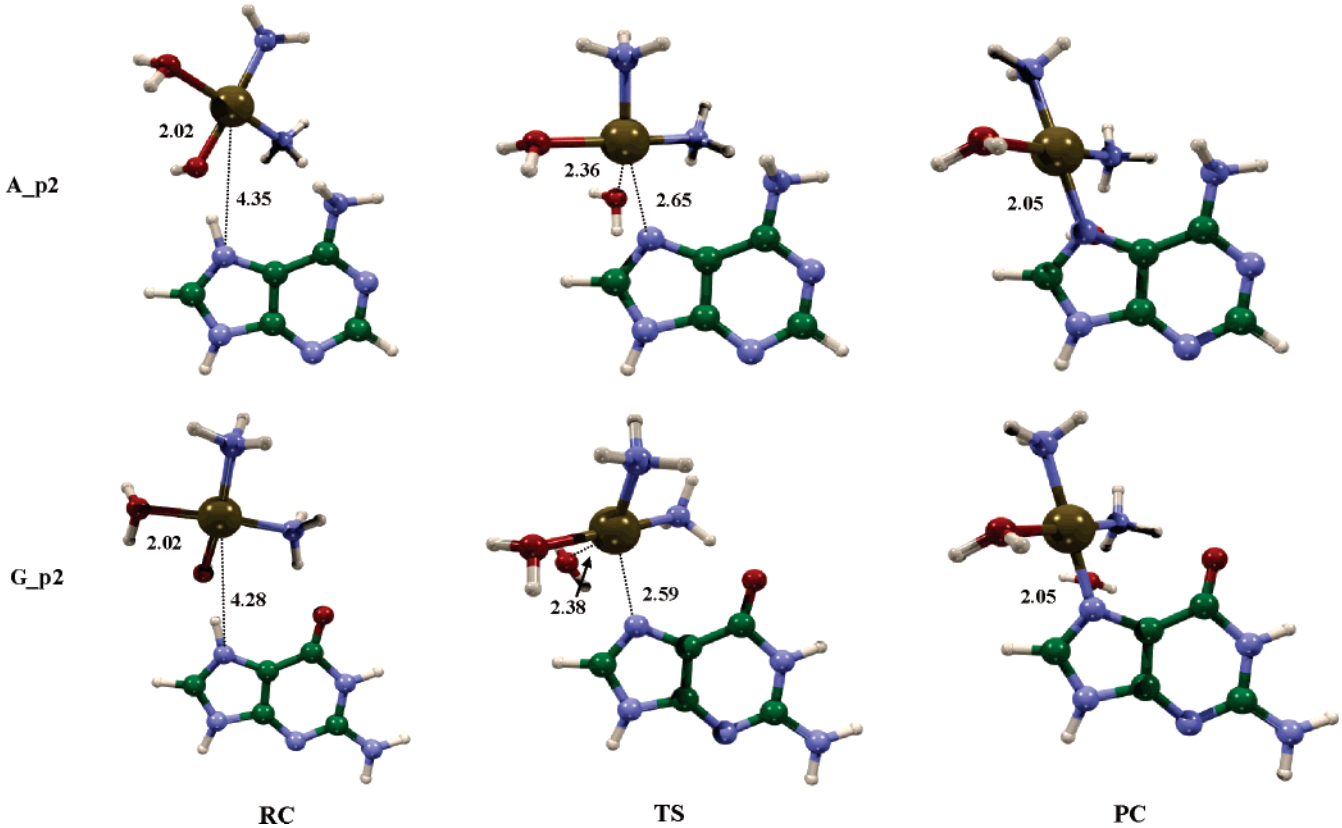

Figure 3. Stationary points (RC, TS, and PC) along the reaction coordinate of the first substitution path 2. Top row shows the substitution of a cisplatin water ligand by adenine, and bottom row shows the substitution with guanine as the attacking ligand.

shorter distance between the leaving ligand and platinum for path 2. The angles between entering and leaving ligands (N7−Pt−O) are in the range of 68−70° for all systems, and the equatorial ligands of the trigonal bipyramid form a plane with the coordinating platinum, in accordance with the theory for substitutions in square planar complexes. The partial proton transfer observed in the G•p1 TS does not significantly alter the C−O bond length of the guanine carbonyl oxygen group

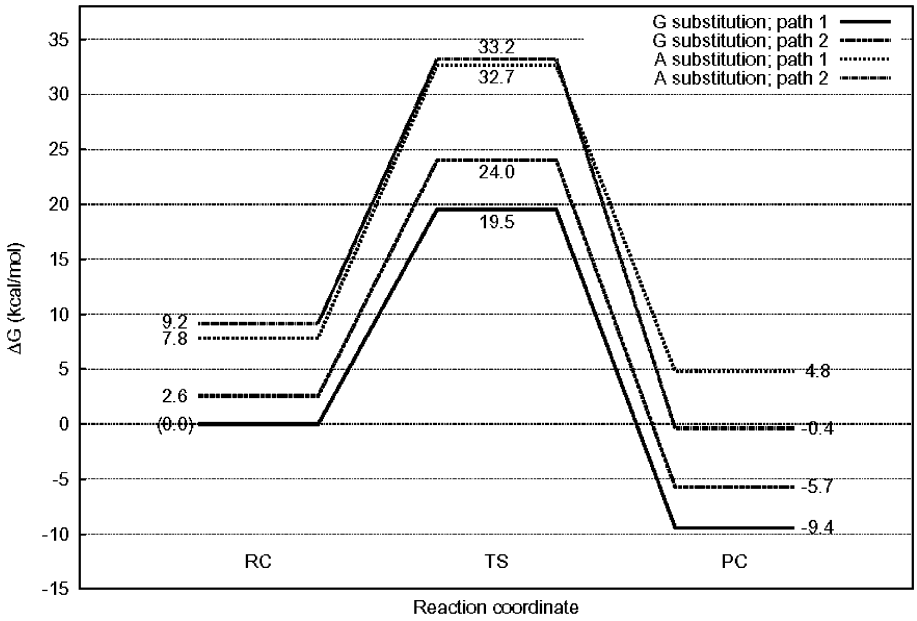

Figure 4. Computed relative Gibbs free energies of the first ligand substitution of diaquated cisplatin.

TABLE 1: Total Energy Composition of the First Substitution Paths with Adenine (A) or Guanine (G)

		SP energy (a.u.)[a]		ΔG_{vib} (a.u.)[b]		ΔG_{solv} (kcal/ mol)[c]	
state	substituent	path 1	path 2	path 1	path 2	path 1	path 2
RC	A	−852.259690	−852.251975	0.201339	0.199032	−168.93	−170.98
	G	−927.566379	−927.557585	0.204376	0.202516	−161.04	−162.83
TS	A	−852.210931	−852.200078	0.199756	0.199896	−173.70	−180.05
	G	−927.521776	−927.509260	0.201291	0.202244	−167.57	−171.54
PC	A	−852.265337	−852.258523	0.199048	0.198777	−166.98	−176.24
	G	−927.573093	−927.559553	0.204526	0.201379	−166.32	169.16

[a] Single-point energies at the B3LYP/(LanL2DZ + 6-311+G(2d,2p)) level on structures optimized at the B3LYP/(LanL2DZ + 6-31G(d,p)) level. [b] Thermodynamic correction to the single-point energies obtained through frequency calculation at the B3LYP/(LanL2DZ + 6-31G(d,p)) level on the optimized stationary point geometries. [c] Solvation energy corrections to the single-point energies calculated using the IEF−PCM solvation model at the B3LYP/(LanL2DZ + 6-311+G(2d,2p)) level.

which only increases from 1.24 Å in the RC to 1.26 Å in the TS, and the double-bonded nature of this carbonyl oxygen is thus retained. The TS geometries are overall in very close agreement with previous theoretical work by Baik et al.[33]

Comparing the PC geometries to the corresponding RCs, there is a slight elongation of the platinum−ammine bond trans to the substituted purine which, according to the trans-effect theory, is a reflection of the stronger electron-donating properties of purine over water. A notable geometric feature is observed in the G•p1 PC geometry where the distance between the guanine moiety O_6 and the water oxygen of L_{ax1} is a mere 2.46 Å, indicating a very strong hydrogen bond.

The energy profiles of the paths, shown in Figure 4, include the BSSE-corrected estimates of the differences in complexation energy between the reactant complexes of A•p1 and G•p1, including solvation energy corrections and thermodynamic corrections to the single-point energies. We have set the effect on the total energy due to proton transfer equal for all RCs. The lowest-lying path, G•p1, also has the lowest energy of activation, $\Delta G^{\ddagger}_{G\bullet p1} = 19.5$ kcal/mol, which is in good agreement with the experimentally determined energy of activation 18.3 kcal/mol for guanosine substitution with cisplatin.[57] The result obtained by Baik et al., $\Delta G^{\ddagger} = 21.8$ kcal/mol, is in fair agreement, especially considering that their reactant complexes were not fully optimized. The activation energy we obtain for the G•p2 path, $\Delta G^{\ddagger}_{G\bullet p2} = 21.4$ kcal/mol, deviates more from the value reported by Baik et al. (25.6 kcal/mol). The disagreement between our results and those of Baik et al. increases further for the adenine substitutions where we obtain $\Delta G^{\ddagger}_{A\bullet p1} = 24.8$ kcal/mol and $\Delta G^{\ddagger}_{A\bullet p2} = 24.0$ kcal/mol compared to 34.5 and 37.6 kcal/mol in their study.

This difference is in all likelihood due to the lack of optimized reactant complex geometries in previous work. A contributing factor likely to have some influence on the obtained activation energies is of course also the proton transfers observed here, although these should serve to raise the activation barriers by lowering the RC energy.

Overall, the reactions are exothermic for all substitutions, $\Delta G_{G\bullet p1} = -9.4$ kcal/ mol, $\Delta G_{G\bullet p2} = -8.3$ kcal/mol, $\Delta G_{A\bullet p1} = -3.0$ kcal/mol, and $\Delta G_{A\bullet p2} = -9.5$ kcal/mol. This can be compared to the values reported by Baik et al. for $\Delta G_{A\bullet p1}$ and $\Delta G_{G\bullet p1}$ (−3.4 kcal/mol and −14.4 kcal/mol, respectively), again reflecting the difference in energy of the RCs.

The activation energy profiles obtained herein indicate a different source of the cisplatin preference toward guanine than that reported previously. We conclude that this preference is to a significant degree governed by the rate of reactant complex formation rather than merely the activation energy as proposed earlier. This is illustrated by the difference in energy of formation for the A•p1 and G•p1 RCs which is calculated to be 7.8 kcal/mol in favor of G•p1. It is, however, likely that also the differences in activation energy play a part in cisplatin selectivity toward guanine, given that the average difference in activation energy is ∼4 kcal/mol between adenine and guanine substitutions in these calculations.

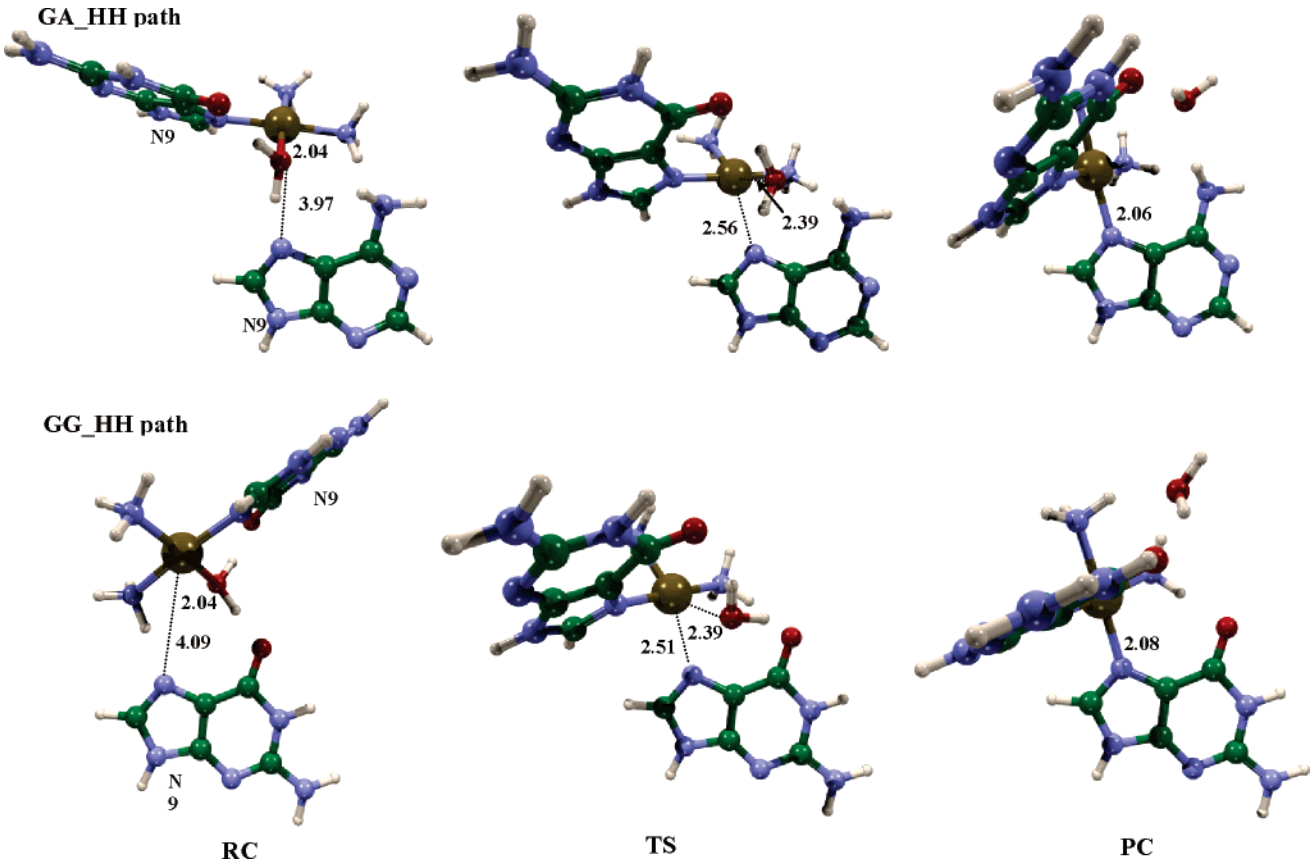

Figure 5. Stationary points (RC, TS, and PC) along the reaction coordinate of the second substitution leading to the head-to-head conformation of the product. Top row shows the substitution with adenine as the attacking ligand, and bottom row show the substitution with guanine as the attacking ligand.

The choice of water as dielectric medium for the PCM calculations is somewhat problematic as the purines in the context of DNA are not fully exposed to the solvent. Furthermore, specific interactions of the model system with surrounding portions of DNA are not accounted for. However, assuming that the DNA surrounding, that is, adjacent bases, of a random adenine on average is the same as that of a random guanine, the choice of solvation model is justified on the basis of cancellation of errors when comparing relative energies of the reactions. This reasoning also applies to the second substitution, assuming that the average DNA surrounding of a GA/AG sequence is equal to that of a GG sequence. The solvation model also highlights the chemical differences of cisplatin substitution with the different purines.

The Second Substitutions. The second substitutions have been studied with the aim of finding product complexes that display the same overall structural features as the experimentally determined cisplatin−DNA didentate adducts, that is, the head-to-head (HH) and the head-to-tail (HT) configurations. Given the preference of guanine binding in the first substitution, and the experimental evidence pointing to guanine being the initial substituent, the reactions studied here are as follow:

$$cis\text{-}Pt[NH_3]_2[H_2O][G]^{2+} + G \rightarrow cis\text{-}Pt[NH_3]_2[G]_2^{2+} + H_2O$$

$$cis\text{-}Pt[NH_3]_2[H_2O][G]^{2+} + A \rightarrow cis\text{-}Pt[NH_3]_2[G][A]^{2+} + H_2O$$

We have calculated the paths leading to HH and HT configurations for both adenine and guanine as the second substituent. The naming convention used for the reactions is (GG, GA)•(HH, HT)•(RC, TS, PC), that is, the reactant complex for the reaction in which the second substitutent is guanine on a path leading to a head-to-head product is denoted GG•HH•RC. In the case of GG•HT, two alternative paths lead to the same principal product geometry, and thus the index 1 or 2 is added.

The reactant complexes are shown in Figures 5 and 6. The reactant complexes starting from the G•p1 product of the first substitution are GG•HH•RC, GG•HT•RC_1, and GA•HH•RC. The reactant complexes starting from G•p2 are GG•HT•RC_2 and GA•HT•RC. The proton transfers observed in the first substitution are absent in the second substitutions, the one exception being GA•HT•RC where a proton of the water ligand is transferred to N7 of adenine.

Both reactions leading to HH conformation and GG•HT•PC_1 stem from the G•p1 reactant moiety, and the rest stem from the G•p2 moiety.

The alignment of the attacking purine to the cisplatin ligands in all cases but one follow the pattern established in the first substitution, that is, N7 of the attacking purine is hydrogen-bonded to the water ligand that is eventually substituted, and the attacking purine O_6/N_6 group is hydrogen-bonded to the ligand in cis position to the water. The exception to this pattern is found in the GG•HH•RC complex where the hydrogen-bonding pattern of the attacking guanine is reversed in that O_6 forms a hydrogen bond to the water and N7 hydrogen bonds to the ammine cis to the water. This RC closely resembles GG•HT•RC_1 but with a flipped orientation of the attacking guanine. On visual inspection of the GG•HH•RC structure (Figure 5) this would seem an unlikely RC geometry for adjacent DNA bases located on the same strand, given that the distance between the guanine N9 atoms in our geometry, in-vivo bonding

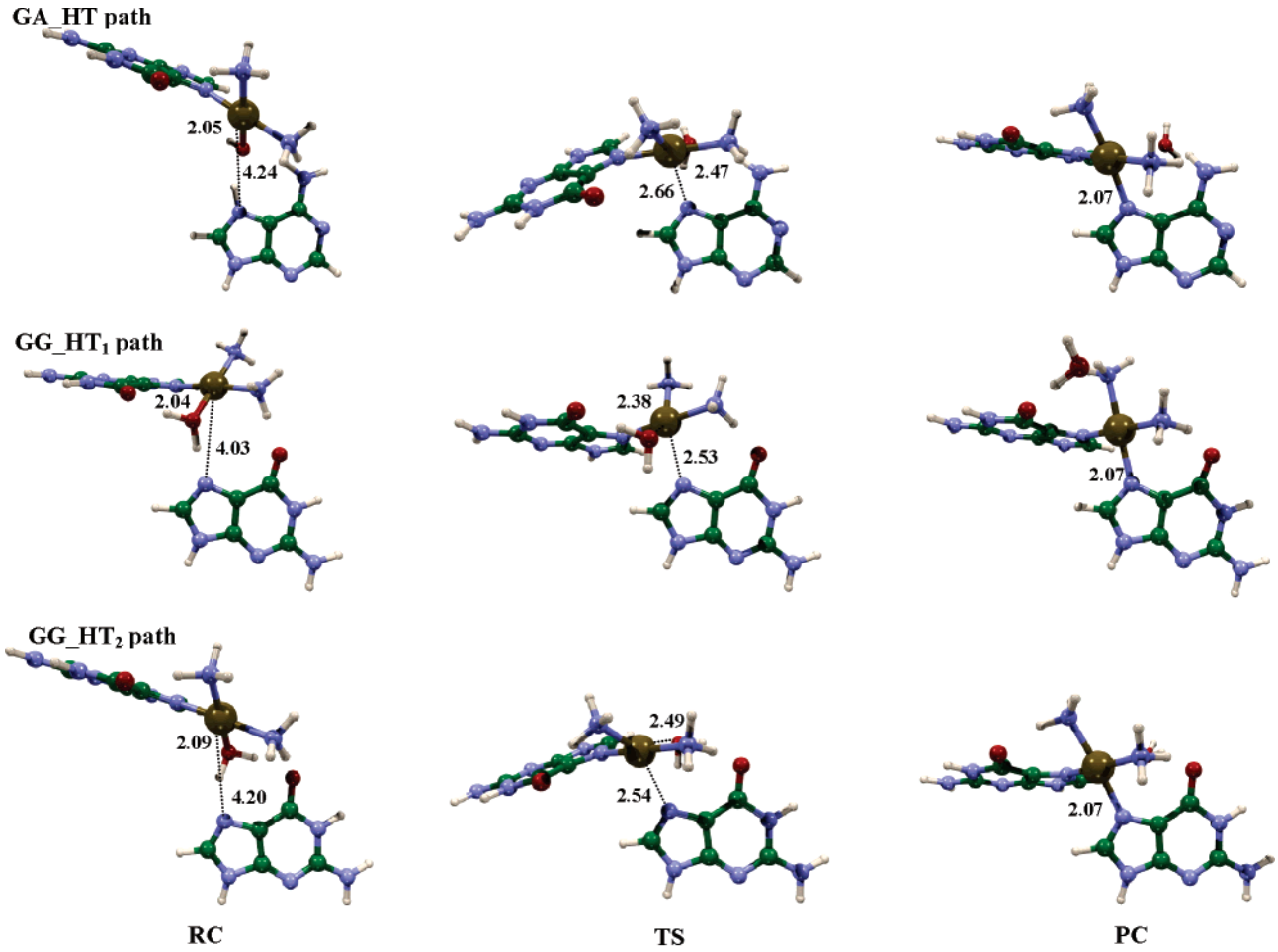

Figure 6. Stationary points (RC, TS, and PC) along the reaction coordinate of the second substitution leading to the head-to-tail conformation of the product. Top row show the adenine substitution. The middle and bottom rows show the two alternative reaction paths leading to a head-to-tail conformation when the substituent is a guanine.

to the ribose of the DNA backbone, is 9.7 Å. To a lesser extent this is also true for the GA•HH•RC, where the distance between the purine N9 atoms is 7.7 Å. This is likely an effect of the model system not accounting for the restraints imposed by the adjoining parts of DNA. It must be kept in mind, though, that the DNA molecule is very flexible and intrastrand didentate adducts are also known to be formed between guanines separated by one nucleotide in the sequence.

To compare the reaction energy profiles of the second substitution, complexation energies were calculated for the GG•HT•RC_1 and GA•HH•RC complexes in the same manner described above for the first substitution. The difference in complexation energy was estimated to 6.6 kcal/mol, with GG•HT•RC_1 having the lower value of the two reactant complexes.

The transition-state geometries of the second substitutions were in all aspects very similar to those of the first substitutions with respect to the primary atoms involved. All TSs are trigonal bipyramids with the equatorial ligands and platinum forming a plane, but with a larger spread in the angles between the attacking purine and the leaving water ligand (between 63° and74°, compared to 68°−70° for the first substitution). Distances between the attacking purine N7 and platinum range between 2.53 and 2.66 Å, and the platinum-to-leaving-water distances range between 2.48 and 2.49 Å. The corresponding TS distances of the first substitution range between 2.59 and 2.65 Å and 2.38−2.50 Å, respectively. The larger variation in the angle between attacking and leaving ligand reflects the restraints imposed by the additional hydrogen bonds and steric interactions present in the second substitution.

The imaginary frequencies are of a low magnitude, as in the first substitution TSs, in the range 144i−175i cm^{-1}.

The flipped hydrogen-bond orientation of GG•HH•RC is in the associated TS reversed, and O_6 of the attacking guanine is now hydrogen-bonded to both the leaving water ligand and the ammine group cis to it, and N7 is oriented toward the platinum atom.

As briefly mentioned above, the product complexes are of two types: head-to-head and head-to-tail. A prototypical HH PCs is of C_S symmetry; for HT PC, C_2 symmetry is observed.

In experimentally determined structures of platinated dsDNA oligomers, the N7 of the platinated purines is observed to be out of the platinum coordination plane.[16,17] This is not observed in the PCs obtained in the calculations and can be attributed to the force exerted on the adduct by the surrounding DNA, in particular the DNA phosphoribose bridge.

The bond distances in the calculated PCs can be compared to experimentally determined structures[16,17] and previous theoretical work by Burda and Leszczynski.[32] These are summarized in Table 2. Compared to the experimental structures, bond lengths obtained through our calculations are on average about 0.20 Å too long, which is in line with the well-known overestimation of metal−ligand bond lengths by the currently employed B3LYP functional. In comparison with the results presented by Burda and Leszczynski, we obtain slightly longer metal−ligand bonds (<0.04 Å longer) due to the different basis

TABLE 2: Bond Lengths (Å) between Platinum and Its Ligands in the Product of the Second Substitution

species	Pt−L_1[a]	Pt−L_2	Pt−L_3	Pt−L_4
GA_HH	2.064 (A)	2.081	2.096	2.098
Pt_a_2AG[b]	2.041 (A)	2.044	2.089	2.095
GG_HT_1	2.070 (G)	2.058	2.100	2.088
GG_HH	2.085 (G)	2.067	2.085	2.092
Pt_a_2G_2[b]	2.065 (G)	2.065	2.074	2.074
1A84[c]	1.925 (G)	1.859	1.902	1.833
1A2E[d]	2.010 (G)	1.991	2.104	2.048

[a] $L_{[1-4]}$ denotes the ligands bonded to Pt. L_1 = A or G; L_2 = G; L_3 = L_4 = ammine. [b] Ref 32. [c] From crystal structure of intrastrand adduct 1,2-d(GpG) (PDB entry 1A84); ref 16. [d] From crystal structure of GG interstrand adduct (PDB entry 1A2E); ref 17.

set used in the optimizations. The presence of the nonbonded water molecule (absent in the study by Burda and Leszczynski) affects the Pt−ligand bond lengths slightly, as seen when comparing the geometries of GG•HT•PC_1 and GG•HT•PC_2, in which the water has a different hydrogen-bonding pattern and position. In these PCs, the Pt−N bond length of the ammine ligand cis to the position of the second substitution differs by 0.02 Å.

A largely influential geometrical factor directing the substitution product toward a HH or HT conformation, suggested on the basis of these calculations, is whether the RC of the second substitution contains a G•p1 or G•p2 moiety. The RCs containing a G•p2 moiety lead to the HT-type product complex, and RCs containing a G•p1 moiety lead to the HH-type product complex. In the exceptional case of GG•HT_1, this may be a consequence of the model system allowing degrees of freedom that would be constrained in a larger model system including surrounding portions of the DNA molecule.

The substitution energy profiles, shown in Figure 7 and Table 3, display small variations with respect to the barrier of activation. In Figure 7, the BSSE-corrected complexation energy difference between the GG and GA paths is included. The GA•HT path has the lowest energy of activation at 21.1 kcal/mol, closely followed by the GG•HT_2 path at 21.2 kcal/mol. In general, the HT paths show slightly lower barriers of activation than the HH paths and are also thermodynamically more favored. This is likely due to less steric interactions in the HT PCs in our model system. The most stable reactant complex is that of the GG•HT_1 path, with the GG•HH reactant complex only 0.3 kcal/mol higher. The experimentally determined value for the barrier of GG adduct closure in dsDNA, 23.4 kcal/mol,[58] is in good agreement with our value for the barrier of the GG•HH path, 22.5 kcal/mol.

Overall, the differences in barrier heights and relative thermodynamic stabilities between reactant and product complexes within a single reaction path are too small to explain the preference for a particular type of didentate platination product, that is, intrastrand 1,2-d(GpG) or 1,2-d(ApG) adducts. Instead, the distinguishing feature directing cisplatins preference toward guanine substitutions, we believe, can be found in the higher thermodynamic stability of reactant complexes with guanine than adenine, both for the first (by 7.8 kcal/mol) and the second substitution (by 6.6 kcal/mol).

Comparing inter- vs intrastrand energy profiles, the computed data suggest that interstrand adduct formation should be favored, on the basis of both the lower barriers (albeit only slightly lower) and more stable product complexes. This discrepancy with experimental evidence can probably be attributed to the model system not accounting for the DNA surrounding, making certain geometrical conformations energetically unfavorable.

Considering the difference in product complex energy of the first guanine substitution (G•p1•PC being 3.7 kcal/mol lower than that of G•p2•PC), it is somewhat surprising to see that the energy difference of comparable reactant complexes in the second substitution are so small, for example, GG complexes containing a G•p1 or G•p2 moiety. Apparently the difference in thermodynamic stability of the first substitution is influenced more by the position of the substituted water than the hydrogen bond formed with the guanine oxo group. Hence, conclusions about the preferred substitution path of the first platination reaction based on thermodynamic stability alone appear highly model system-dependent. One should bear in mind, though, that in the full system there are many water molecules surrounding the adducts, thus able to influence the reactions and stabilities.

Conclusions

We have in the present work performed a mechanistic study of the two sequential substitution reactions of the diaquated form of the anti-tumor drug cisplatin with the DNA bases adenine and guanine, which are the clinical targets of this drug.

In the first substitution, two possible alignments of the purines with respect to the diaquated cisplatin, corresponding to two separate reaction paths, were found. The second substitution employed the two product complexes from the first substitution reaction with guanine (without the substituted water ligand) and either adenine or guanine as second substituents.

The geometries of the stationary points of the first substitution closely agree with previous theoretical work and the established theory for ligand substitution in square planar complexes. The activation energy barrier for path 1 substitution by guanine (19.5 kcal/mol) closely agrees with both experimental measurements (18.3 kcal/mol) and previous theoretical work (21.8 kcal/mol). Barriers of the path 2 guanine substitution and path 1 and 2 adenine substitutions were found to be 21.4, 24.8, and 24.0 kcal/mol, respectively. These results conflict with previous theoretical work where barriers of 25.6, 34.5, and 37.6 kcal/mol were reported. Two main sources of this discrepancy can be distinguished: the differences in basis set employed and the lack of optimized reactant complexes from which to calculate the barrier height in earlier work. All reaction paths are found to be exothermic.

In the study by Baik et al.,[33] the bias of cisplatin toward guanine substitution is concluded to depend on the activation energy barrier alone. The current work instead suggests that the preference of cisplatin toward substitution with guanine over adenine is governed by the thermodynamic stability of reactant complex formation in combination with a higher energy of activation for the adenine substitution. The complexation energy difference was calculated to be 7.8 kcal/mol in favor of guanine.

The reactants in the second substitutions are adenine or guanine as attacking ligand and cisplatin−guanine product complexes of the first substitution. The aim of studying this substitution was to find the discriminating factors directing the reaction toward the head-to-head (HH) or head-to-tail (HT) configuration of the final product, corresponding to intra- and interstrand adducts, respectively, as found in experimental studies. In addition, this allowed for the origin of the preference for guanine over adenine in the second substitution to be addressed.

Several paths leading to HH and HT product conformations were found for both adenine and guanine, and for the guanine substitution leading to HT configuration, two different paths were located. In general, the HT products stem from reactions starting with the G•p2 product complex as one of the reactants,

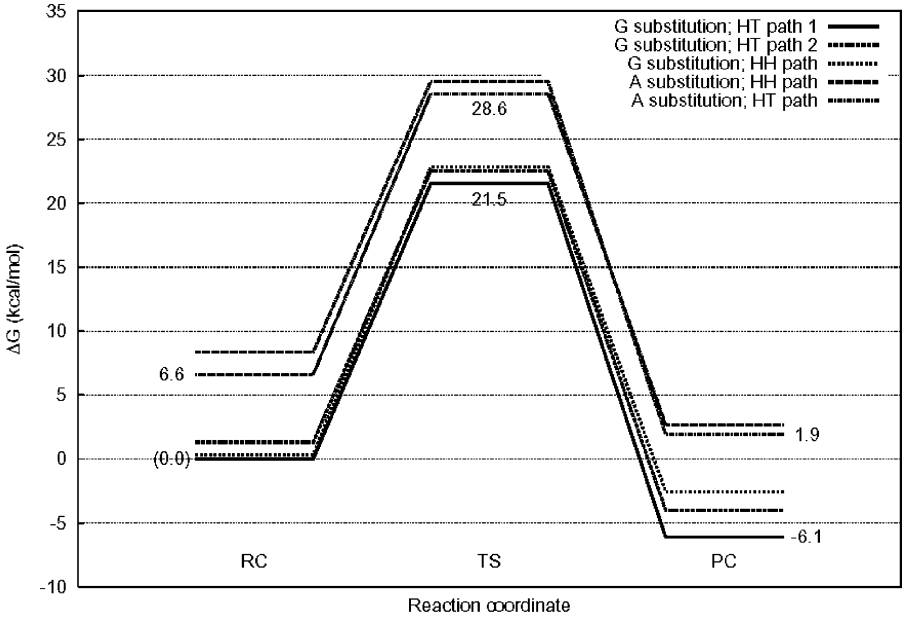

Figure 7. Computed relative Gibbs free energies of the second ligand substitution of diaquated cisplatin.

TABLE 3: Total Energy Composition of the Second Substitution HH and HT Paths with Adenine (A) or Guanine (G)

		SP energy (a.u.)[a]		ΔG_{vib} (a.u.)[b]		ΔG_{solv} (kcal/ mol)[c]	
state	substituent	HH	HT	HH	HT	HH	HT
RC	A	−1318.592637	−1318.598570	0.284867	0.285262	−160.94	−155.70
	G	−1393.889596	−1393.891080[d]	0.286406	0.286330[d]	−154.77	−154.13[d]
			−1393.897086[e]		0.289085[e]		−150.77[e]
TS	A	−1318.554460	−1318.554812	0.286322	0.285132	−163.84	−161.94
	G	−1393.853448	−1393.854139[d]	0.289569	0.287437[d]	−156.96	−156.48[d]
			−1393.856851[e]		0.289380[e]		−154.99[e]
PC	A	−1318.603041	−1318.605862	0.285841	0.285489	−158.96	−157.74
	G	−1393.900127	−1393.903900[d]	0.288557	0.287211[d]	−152.41	−152.74[d]
			−1393.899265[e]		0.288099[e]		−154.10[e]

[a] Single-point energies at the B3LYP/(LanL2DZ + 6-311+G(2d,2p)) level on structures optimized at the B3LYP/(LanL2DZ + 6-31G(d,p)) level. [b] Thermodynamic correction to the single-point energies obtained through frequency calculation at the B3LYP/(LanL2DZ + 6-31G(d,p)) level on the optimized stationary point geometries. [c] Solvation energy corrections to the single-point energies calculated using the IEF−PCM solvation model at the B3LYP/(LanL2DZ + 6-311+G(2d,2p)) level. [d] Entry refers to head-to-tail path 1. [e] Entry refers to head-to-tail path 2.

whereas reactant complexes containing the G•p1 product complex lead to the HH arrangement. The geometries of the stationary points of the second substitutions were found to be in agreement with previous theoretical and experimental studies.

As in the first substitution, the reactions of the second substitution were found to be slightly exothermic, with products in the HT configuration being energetically favored over the HH configuration. This is likely an effect of the smaller steric hindrance of the HT configuration in our model system and does not necessarily represent the situation in vivo. The activation energy of the different reaction paths are surprisingly similar (21.1−22.5 kcal/mol) and should thus not constitute the discriminating factor explaining cisplatin's bias toward intrastrand GG adducts. There is good reason to believe the calculated barrier heights to be accurate given that the experimentally determined value for GG adduct closure, 23.4 kcal/mol, agrees well with our computed value for the corresponding reaction (22.5 kcal/ mol). The data obtained for the complexation energy difference between the adenine and guanine reactant complexes of the second substitution (6.6 kcal/mol, favoring guanine complex formation) suggest that again the rate of reactant complex formation strongly influences which didentate adduct is finally observed.

The observed 5′−3′ directionality of 1,2-d(ApG) adducts can be explained by the predominance of initial complex stabilization and binding to guanine. For the second substitution, the DNA geometry allows for binding in the 5′-direction only, and hence only 1,2-d(ApG) is formed. Had initial substitution favored adenine, the geometry of DNA had instead biased the system toward 1,2-d(GpA) 5′−3′ adducts. The larger complex stabilization for G over A in the second substitution furthermore enables more of 1,2-d(GpG) to be formed over 1,2-d(ApG), as the latter interaction will be weaker and associated with a slower reaction rate, thereby having a higher tendency of being removed enzymatically or through hydrolysis prior to adduct closure.

Acknowledgment. The Swedish science research council (VR) and the IVAX Scandinavia research fund are gratefully acknowledged for financial support. We also acknowledge grants of computing time at the supercomputing facilities in Linköping (NSC) and Stockholm (PDC).

References and Notes

(1) Rosenberg, G.; Van Camp, L.; Krigas, T. *Nature* **1965**, *205*, 698.
(2) Loehrer, P. J.; Einhorn, L. H. *Ann. Intern. Med.* **1984**, *100*, 704.
(3) Giaccone, G. *Drugs* **2000**, *59* (Suppl. 4), 9.
(4) Reedijk, J. *Chem. Commun*. **1996**, 801.
(5) Lebwohl, D.; Canetta, R. *Eur. J. Cancer* **1998**, *34*, 1522.
(6) Cleare, M. J.; Hoeschele, J. D. *Plat. Met. Rev.* **1973**, *17*, 3.
(7) Cleare, M. J.; Hoeschele, J. D. *Bioinorg. Chem.* **1973**, *2*, 187.
(8) Reedijk, J. *Inorg. Chim. Acta* **1992**, *198*−*200*, 873.

(9) Wong, E.; Giandomenico, C. M. *Chem. Rev.* **1999**, *99*, 2451.
(10) Beck, D. J.; Brubaker, R. R. *J. Bacteriol.* **1973**, *116*, 1247.
(11) Brouwer, J.; van de Putte, P.; Fichtinger-Schepman, A. M. J.; Reedijk, J.; *Proc. Natl. Acad. Sci.* **1981**, *78*, 7010.
(12) Beck, D. J.; Popoff, S.; Sancar, A.; Rupp, W. D. *Nucleic Acids Res.* **1985**, *13*, 7395.
(13) Eastman, A. *Biochemistry* **1986**, *25*, 3912.
(14) Fichtinger-Schepman, A. M. J.; van Oosterom, A. T.; Lohman, P. H. M.; Berends, F. *Cancer Res.* **1987**, *47*, 3000.
(15) Lepre, C. A.; Strothkamp, K. G.; Lippard, S. J. *Biochemistry* **1987**, *26*, 5651.
(16) Takahara, P. M.; Rosenzweig, A. C.; Frederick, C. A.; Lippard, S. J. *Nature* **1995**, 377, 649.
(17) Coste, F.; Malinge, J.-M.; Serre, L.; Shepard, W.; Roth, M.; Leng, M.; Zelwer, C. *Nucleic Acids Res.* **1999**, *27*, 1837.
(18) Grosschedl, R.; Giese, K.; Pagel, J. *Trends Genet.* **1994**, *10*, 94.
(19) McA'Nulty, M. M.; Lippard, S. J. In *Nucleic Acids and Molecular Biology*; Eckstein, F., Lilley, D. M. J., Eds.; Springer-Verlag: Berlin, 1995; Vol. 9, p 687.
(20) Pil, P. M.; Lippard, S. J. *Science* **1992**, *256*, 234.
(21) Davies, M. S.; Berners-Price, S. J.; Hambley, T. W. *Inorg. Chem.* **2000**, *39*, 5603.
(22) De Bolster, M. W. G.; Cammack, R.; Coucouvanis, D. N.; Reedijk, J.; Veeger, C. *J. Biol. Inorg. Chem.* **1996**, *1*, G1.
(23) Legendre, F.; Bas, V.; Kozelka, J.; Chottard, J.-C. *Chem. Eur. J.* **2000**, *6*, 2002.
(24) Douglas, B.; McDaniel, D. H.; Alexander, J. J. In *Concepts and Models of Inorganic Chemistry*; John Wiley & Sons Inc., New York, 1983.
(25) Hall, A. J.; Satchell, D. P. N. *J. Chem. Soc., Dalton Trans.* **1977**, 1403.
(26) Burda, J. V.; Sponer, J.; Leszczynski, J. *Phys. Chem. Chem. Phys.* **2001**, *3*, 4404.
(27) Spiegel, K.; Rothlisberger, U.; Carloni, P. *J. Phys. Chem. B* **2004**, *108*, 2699.
(28) Zeizinger, M.; Leszczynski, J. *Phys. Chem. Chem. Phys.* **2004**, *6*, 3585.
(29) Robertazzi, A.; Platts, J. A. *Inorg. Chem.* **2005**, *44*, 267.
(30) Deubel, D. V. *J. Am. Chem. Soc.* **2004**, *126*, 5999.
(31) Carloni, P.; Sprik, M.; Andreoni, W. *J. Phys. Chem. B* **2000**, *104*, 823.
(32) Burda, J. V.; Leszczynski, J. *Inorg. Chem.* **2003**, *42*, 7162.
(33) Baik, M.-H.; Friesner, R. A.; Lippard, S. J. *J. Am. Chem. Soc.* **2003**, *125*, 14082.
(34) Zhang, Y.; Guo, Z.; You, X.-Z. *J. Am. Chem. Soc.* **2001**, *123*, 9378.
(35) Costa, L. A. S.; Rocha, W. R.; DeAlmeida, W. B.; Dos Santos, H. F. *J. Chem. Phys.* **2003**, *188*, 10584.
(36) Burda, J. V.; Zeizinger, M.; Leszcsynski, J. *J. Chem. Phys.* **2004**, *120*, 1253.
(37) Robertazzi, A.; Platts, J. A. *J. Comput. Chem.* **2004**, *25*, 1060.
(38) Raber, J.; Zhu, C.; Eriksson, L. A. *Mol. Phys.* **2004**, *102*, 2537.
(39) Becke, A. D. *J. Chem. Phys.* **1993**, *98*, 5648.
(40) Lee, C.; Yang, W.; Parr, R. G. *Phys. Rev. B* **1988**, *37*, 785.
(41) Hay, P. J.; Wadt, W. R. *J. Chem. Phys.* **1985**, *82*, 270.
(42) Wadt, W. R.; Hay, P. J. *J. Chem. Phys.* **1985**, *82*, 284.
(43) Hay, P. J.; Wadt, W. R. *J. Chem. Phys.* **1985**, *82*, 299.
(44) Gonzales, C.; Schlegel, H. B. *J. Chem. Phys.* **1989**, *90*, 2154.
(45) Gonzales, C.; Schlegel, H. B. *J. Phys. Chem.* **1990**, *94*, 5523.
(46) Mennucci, B.; Tomasi, J. *J. Chem. Phys.* **1997**, *106*, 5151.
(47) Mennucci, B.; Cancs, E.; Tomasi, J. *J. Phys. Chem B* **1997**, *101*, 10506.
(48) Tomasi, J.; Mennucci, B.; Cancs, E. *J. Mol. Struct. (THEOCHEM)* **1999**, *464*, 211.
(49) Simon, S.; Duran, M.; Dannenberg, J. J. *J. Chem. Phys.* **1996**, *105*, 11024.
(50) Boys, S. F.; Bernardi, F. *Mol. Phys.* **1970**, *19*, 553.
(51) Zhu, C.; Raber, J.; Eriksson, L. A. *J. Phys. Chem. B*, in press.
(52) Frisch, M. J.; Trucks, G. W.; Schlegel, H. B.; Scuseria, G. E.; Robb, M. A.; Cheeseman, J. R.; Montgomery, J. A., Jr.; Vreven, T.; Kudin, K. N.; Burant, J. C.; Millam, J. M.; Iyengar, S. S.; Tomasi, J.; Barone, V.; Mennucci, B.; Cossi, M.; Scalmani, G.; Rega, N.; Petersson, G. A.; Nakatsuji, H.; Hada, M.; Ehara, M.; Toyota, K.; Fukuda, R.; Hasegawa, J.; Ishida, M.; Nakajima, T.; Honda, Y.; Kitao, O.; Nakai, H.; Klene, M.; Li, X.; Knox, J. E.; Hratchian, H. P.; Cross, J. B.; Adamo, C.; Jaramillo, J.; Gomperts, R.; Stratmann, R. E.; Yazyev, O.; Austin, A. J.; Cammi, R.; Pomelli, C.; Ochterski, J. W.; Ayala, P. Y.; Morokuma, K.; Voth, G. A.; Salvador, P.; Dannenberg, J. J.; Zakrzewski, V. G.; Dapprich, S.; Daniels, A. D.; Strain, M. C.; Farkas, O.; Malick, D. K.; Rabuck, A. D.; Raghavachari, K.; Foresman, J. B.; Ortiz, J. V.; Cui, Q.; Baboul, A. G.; Clifford, S.; Cioslowski, J.; Stefanov, B. B.; Liu, G.; Liashenko, A.; Piskorz, P.; Komaromi, I.; Martin, R. L.; Fox, D. J.; Keith, T.; Al-Laham, M. A.; Peng, C. Y.; Nanayakkara, A.; Challacombe, M.; Gill, P. M. W.; Johnson, B.; Chen, W.; Wong, M. W.; Gonzalez, C.; Pople, J. A. Gaussian 03, Revision B.02; Gaussian, Inc.: Pittsburgh, PA, 2003.
(53) Zoltewicz, J. A.; Clark, D. F.; Sharpless, T. W.; Grahe, G. *J. Am. Chem. Soc.* **1970**, *92*, 1741.
(54) Yanagawa, H.; Ogawa, Y.; Ueno, M. *J. Biol. Chem.* **1992**, *267*, 13320.
(55) Li, X.-Y.; McClure, W. R. *J. Biol. Chem.* **1998**, *273*, 23558.
(56) Baik, M.-H.; Friesner, R. A.; Lippard, S. J. *J. Am. Chem. Soc.* **2002**, *124*, 4495.
(57) Arpalahti, J.; Lippert, B. *Inorg. Chem.* **1990**, *29*, 104.
(58) Bancroft, D. P.; Lepre, C. A.; Lippard, S. J. *J. Am. Chem. Soc.* **1990**, *112*, 6860.